Challenges in ground-truthing magnetizations interpreted from magnetic field data

Austin, J.R. [1], Foss, C. A. [2], Clark, D. A. [3] & Patterson, B.O. [1]

1. Multiphysics, CSIRO Mineral Resources
2. Geophysics of Cover, CSIRO Mineral Resources
3. Superconducting Systems and Devices Group, CSIRO Manufacturing & CSIRO Mineral Resources

ABSTRACT

Lack of confidence in palaeomagnetic data related to spurious magnetizations, and the difficulties relating to upscaling of palaeomagnetic measurements represent significant challenges to palaeomagnetic data being more widely used to constrain magnetic field data. Inversions of magnetic field data measured at a considerable distance from a magnetic source, i.e., airborne TMI data, provide a constraint of the total magnetization (in terms of intensity and direction), but provide little information about its exact distribution or its possible internal inhomogeneity. Even where samples are available to directly measure both magnetic susceptibility and remanent magnetization (which in combination produce the resultant magnetization giving rise to the external magnetic anomaly), there are considerable challenges to quantitatively explain a magnetic anomaly with reference to those measures of sub-surface magnetization. Challenges arise partly through presence of spurious magnetizations which may be caused by a number of phenomena. Samples collected from the surface are prone to lightning strikes that cause lightning induced remanences, specimens obtained from diamond drill core are prone to drilling-induced magnetizations, and any samples can be contaminated by magnetizations induced from pencil magnets. With enough data it is possible to identify such overprints through step-wise magnetic cleaning of the samples, but their removal still leaves questions about the original magnetization of the rock. Another major challenge arises from the density at which a geological body is sampled, and whether that data can be up-scaled sufficiently to capture the inhomogeneity of the geological body that gives rise to a magnetic anomaly. Both magnetic susceptibility and remanent magnetization measured in what may be considered a single geological unit can vary considerably and with low predictability across a wide range of scales. Some bodies are more complex than others, and require increased density of sampling. However, most critically, recognizing the limitations of the way in which palaeomagnetic data are sampled is critical to our confidence in understanding magnetizations within geological bodies.

INTRODUCTION

In theory, it is optimal to constrain potential field modelling procedures using measured petrophysical data. However, it is not always possible or feasible to do so. For example, where the units in question are recessive and/or weathered at surface. Even where units do crop out, it may be difficult to obtain permission to sample them. Furthermore, where rocks can be sampled there are a number of artificial overprints that may cause confusion to interpreters. The most common of these are drilling-induced magnetization, overprinting by pencil magnets, and lightning-induced magnetization. Even where the modelled lithologies can be constrained by petrophysical measurements, the calculation of bulk properties that are representative of a given body overall, from those limited samples can be highly problematic. In this study we explore some of the challenges in ground-truthing magnetizations interpreted from magnetic field data.

DRILLING INDUCED MAGNETIZATION

Drilling induced magnetization (DIM) is a class of isothermal remanent magnetization, which is common in multidomain (MD) grains (Audunsson and Levi, 1989), i.e., it tends to mostly overprint VRM (viscous remanent magnetization). It occurs when the upward magnetic field is deflected into the orientation of the drill rod (Fig 1). Then, during drilling, vibrations and/ or heat associated with grinding the rock at the drill bit demagnetize the rock. The rock then re-magnetizes in the field inside the rod, and acquires remanence in the rod orientation.

DIM totally to partially re-magnetizes a sample such that the measured NRM directions tend to parallel the drilling orientation. In the southern hemisphere the magnetization vector is usually anti-parallel to the drill string plunge (i.e., upward oriented), whereas in the northern hemisphere it is generally parallel (i.e., downward oriented).

Figure 1: Schematic Illustration of how drilling induced magnetization is acquired.

Zone	Area	J (A/m)	J per area (A)
1	3.14	1	3.14
2	9.42	1.5	14.14
3	15.71	2.5	39.27
4	21.99	3.5	76.97
5	28.27	4.5	127.23
Total	**78.54**	**3.32**	**260.75**

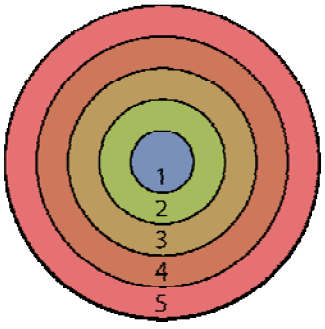

Figure 2: Results of a basic calculation used to estimate the increase in intensity of NRM due to drilling induced magnetization (DIM). In this calculation there is a linear increase in magnetization from the core of the sample to the outer edge of 5, and this corresponds approximately to an enhancement due to DIM of ~3.3 times *in situ* NRM.

There are at present only a few suitable datasets that can give us a quantifiable perspective on exactly how much DIM enhances the NRM intensity of a given rock. A study by Audunsson and Levi (1989), showed that the DIM intensity within a single sample increased by at least a factor of five from the center of the drill core to the drill string's cutting surface, where it appears to have been produced. If we use this observation as a starting hypothesis, and assuming a linear decline in the intensity of DIM from the edge of the core to the center (where there is zero enhancement) we can make a rough calculation of the intensity of the DIM relative to the area of the core (in cross-section) as shown in Figure 2. Although this is a very approximate calculation, what it does suggest is that there should be an increase in the NRM intensity by a factor of approximately 3.3 on average for rocks affected by DIM. This is a reasonably conservative estimate, given that De Wall and Worm (2001) suggested that the increase in DIM from core to the outer core surface could be closer to a factor of ten.

A limited study was completed on some magnetite-rich samples of ore from the Monakoff mine. Some of the samples were obtained via surface drilling using a handheld alloy barreled drill by Austin, Schmidt and Lilly (2013), and others were extracted from a section of core produced by a conventional diamond drill rig (collected as part of this study). The samples were checked using a Tescan Integrated Mineral Analyser (TIMA) to ensure that they have approximately comparable mineralogy and grain size, and it was confirmed that both have a similar texture with similar mineralogy, consisting mainly of barite, magnetite, chalcopyrite, and sphalerite (Figure 3).

Density, magnetic susceptibility, NRM and Koenigsberger ratios of the samples were then compared using a number of graphs (Figure 4 a-i; a-c being samples collected at the surface, g-i being samples affected by DIM). The results from both DIM affected samples and surface sampled specimens were averaged and are plotted relative to each other in Figure 4 d-f. The averaged results of density and magnetic susceptibility are comparable for both subsets of data, with density of approximately 4 g/cc, and magnetic susceptibility of approximately 0.5 SI (Fig 4d). This indicates that they have approximately equal proportions of magnetite on average. However, the same datasets show a large disparity in the average NRM and also Koenigsberger ratio. What the results appear to show, is that the DIM affected samples have NRM that is approximately 3 times stronger than for very similar samples that are not affected by DIM. These measurements are consistent with the observations of Audunsson and Levi (1989).

These results should be used to evaluate the remanent magnetization data presented in any study where samples have been extracted from diamond drill core. Any instances of extreme remanent magnetization should be treated with caution, and it should be assumed that the NRM values may be enhanced by DIM to somewhere in the order of 2 - 5 times the pre-drilling NRM intensity. Furthermore, DIM affected magnetizations will not be representative of the pre-drilling NRM direction either.

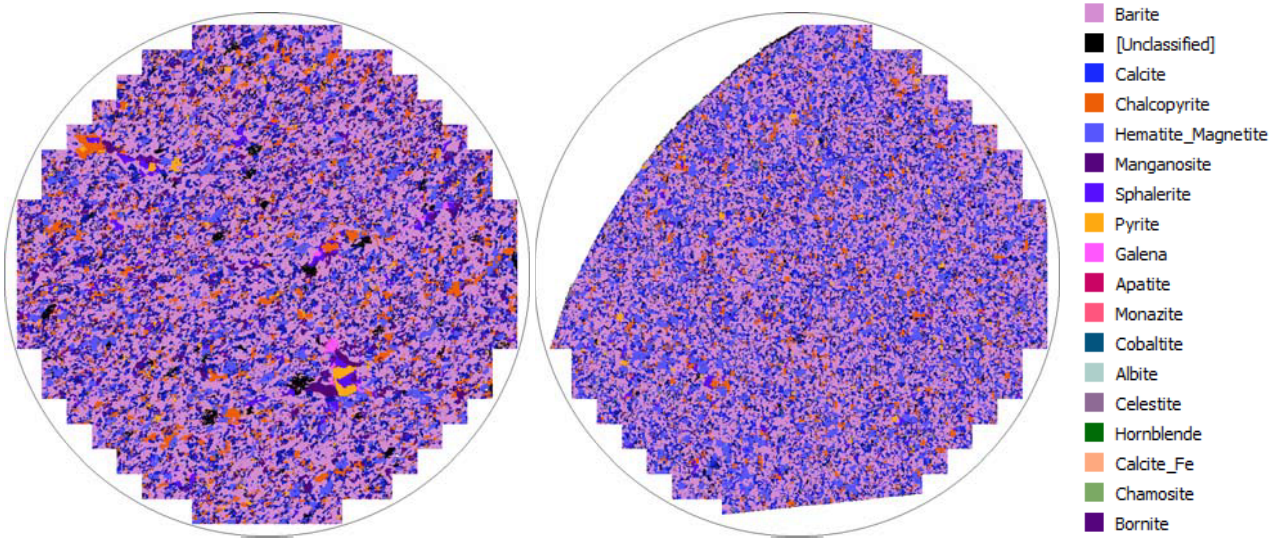

Figure 3: Shows TIMA scans of two of the samples included in the study, MNK003 (drilled at surface) and MON005 (sampled from Diamond Drill core). Note that the mineralogy is very similar and the grainsize is comparable. Field of view = 21 mm.

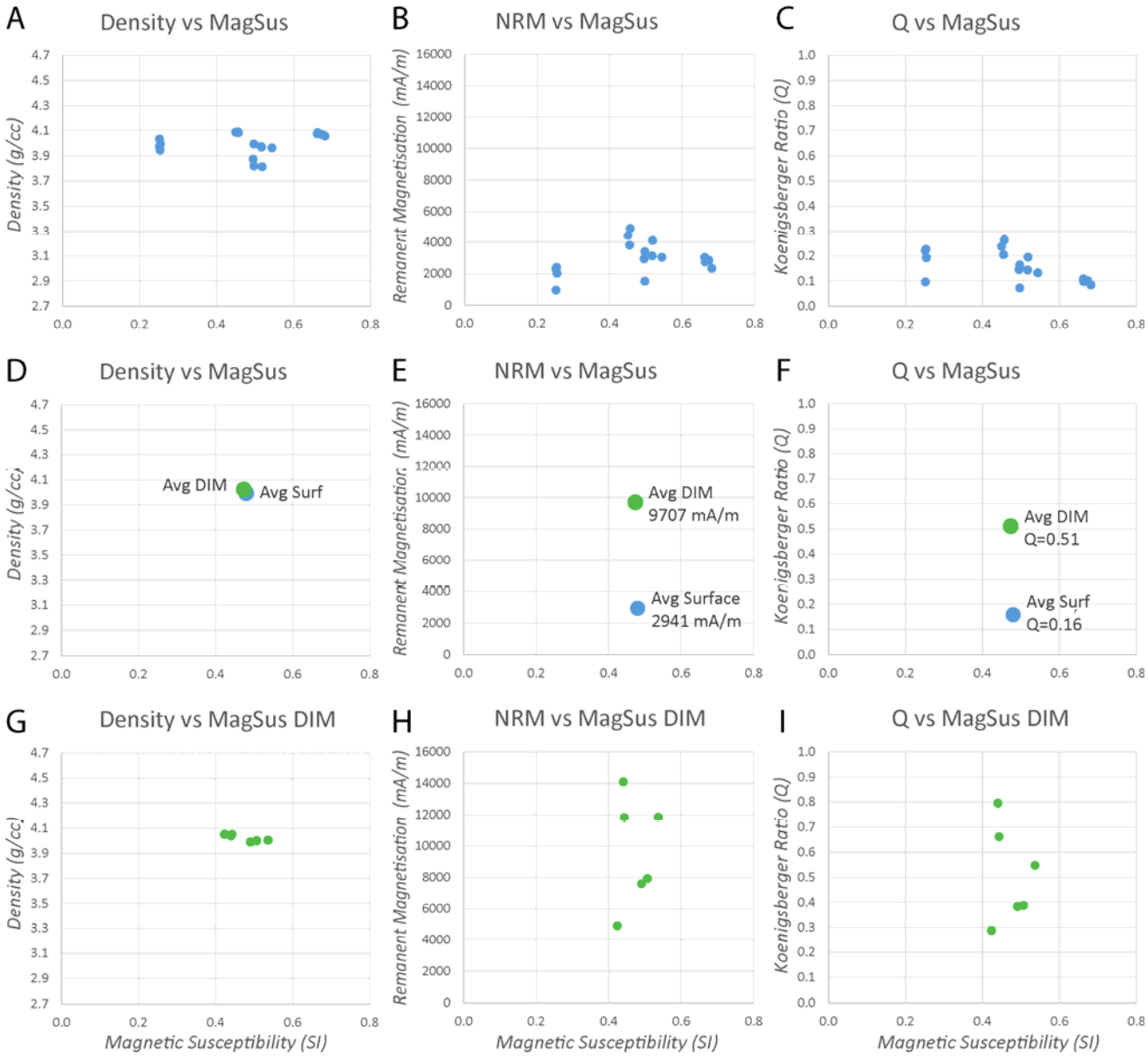

Figure 4: A series of graphs detailing the petrophysical properties of a set of comparable samples of barite-magnetite-chalcopyrite ore from the Monakoff Mine. A-C are samples obtained from the surface; g-i are samples collected from diamond drill core (DIM affected) and the average results are plotted in d-f.

PENCIL MAGNETS

Pencil magnets are commonly used by geologists to assess whether magnetic minerals, e.g., magnetite or pyrrhotite, are present within core samples. Unbeknownst to most, the act of placing a magnet on the core exposes the core to a large magnetic field. So, ironically, the better the job the geologists does in assessing the core, the more likely it is to be contaminated from a palaeomagnetic perspective. We measured the magnetic field from a pencil magnet using a shielded fluxgate magnetometer. The results indicate an expected field at the sensor, of the order of 1 Tesla, or roughly 2000 times stronger than the Earth's magnetic field (for mid-latitudes). Such a field is capable of re-magnetizing magnetic minerals within core samples, particularly grains with low coercivity (e.g., multidomain magnetite and pyrrhotite), but furthermore is strong enough to re-magnetize grains with moderate

coercivity (e.g., pseudo single-domain grains). To illustrate this point we applied a pencil magnet to different parts of a degaussed pyrrhotite-rich sample (MT02A) from the Cormorant prospect in the Cloncurry District (e.g., Austin et al., 2016a). The NRM of the sample was measured after each stage, and the sample was degaussed again. The results (Fig 5) illustrate the effect of the pencil magnet on remanent magnetization within the core. In each case the magnet induces a magnetization that is approximately opposite to the position in which the magnet was placed. We can only speculate as to why the magnetization was not exactly opposite, but possible explanations may include: there is a component of stable remanent magnetization still present within the rocks; the polarity of the magnet is not parallel to the shaft of the pencil magnetic; or the magnetic grains may have an anisotropy.

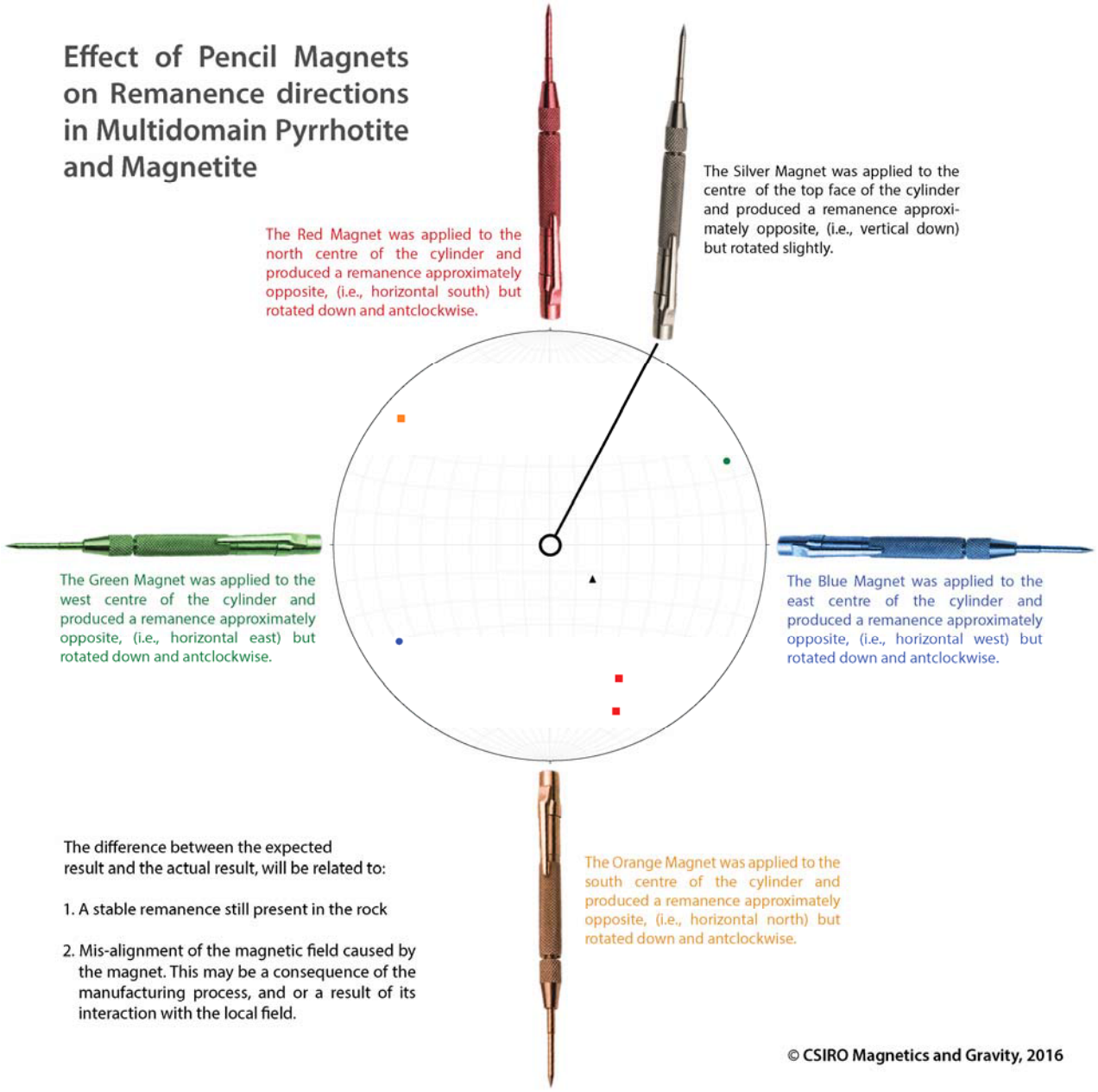

Figure 5: Schematic illustrating the magnetization induced in a low coercivity degaussed specimen, by placing a pencil magnet at different position or the core. The axis of the cylinder is vertical in this case.

Generally speaking, the magnetization of low coercivity samples will be either re-magnetized to the Earth's local magnetic field (for surface drilled or block samples), or to the upward projection of the drill string orientation vector (for rig drilled samples). So the presence of these pencil magnet induced magnetizations is really only a nuisance, making it more difficult to discriminate low coercivity noise from real palaeomagnetic signals. Furthermore, it is usually fairly straight forward to identify the effects of pencil magnets, and if there is any doubt, a simple experiment on the samples using a pencil magnet.

In rig-drilled samples, the characteristic that allows easy identification of PIM, is that there will generally be a large variation in the declination of the magnetizations measured, but all the magnetization directions will be approximately normal to the drill string orientation. For example in samples with pyrrhotite-rich mineralogy from the Artemis prospect (Fig 6; Austin et al., 2016b), several (e.g., ART001D, 023A, 006A, 007A and 025A) have magnetizations approximately normal to the drilling orientation, indicating pencil magnet contamination, and one (ART005A) retains a drilling induced magnetization.

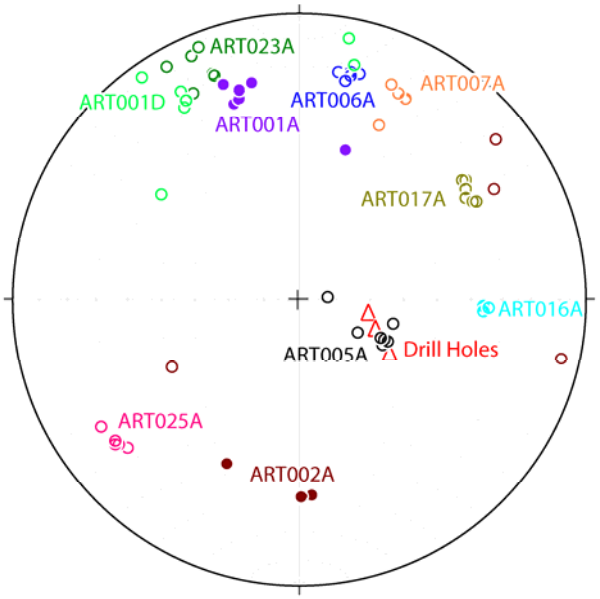

Figure 6: Stereonet displaying the orientations of NRMs and limited demagnetization data for samples from the Artemis prospect. The upward projection of the drill holes is also shown. From Austin et al., 2016b.

LIGHTNING INDUCED MAGNETISATION

Lightning-induced isothermal remanent magnetisation (IRM) is likely to affect surface rocks, especially where they have been sampled from a relative topographic high. The effects usually include elevated remanent magnetisation intensity in lithologically similar samples, often in the order of approximately 5 times the background magnetisation, as illustrated by figure 7, which shows an isolated lightning affected sample compared with a number of unaffected samples.

Where there are sufficient unaffected data, it is usually straight forward to identify the affected samples, but it can be difficult where the rocks display significant geochemical and or textural variation, or have undergone significant deformation. Once a sample is affected by lightning induced magnetisation (LIM) it commonly takes high AF fields (>50 mT) or low temperature demagnetisation to demagnetise the sample sufficiently to deduce a primary magnetisation direction (if this can be done at all). The degree to which rocks are affected by lightning will be determined by their proximity to the strike, but also the geometry of the flow of positive current through the earth and into the atmosphere, as illustrated by Figure 8. Work by Beard et al., 2009, demonstrated that lightning strikes usually only affect radius of 10-30 m from the strike site, and that they cause distinctive starfish shaped anomalies.

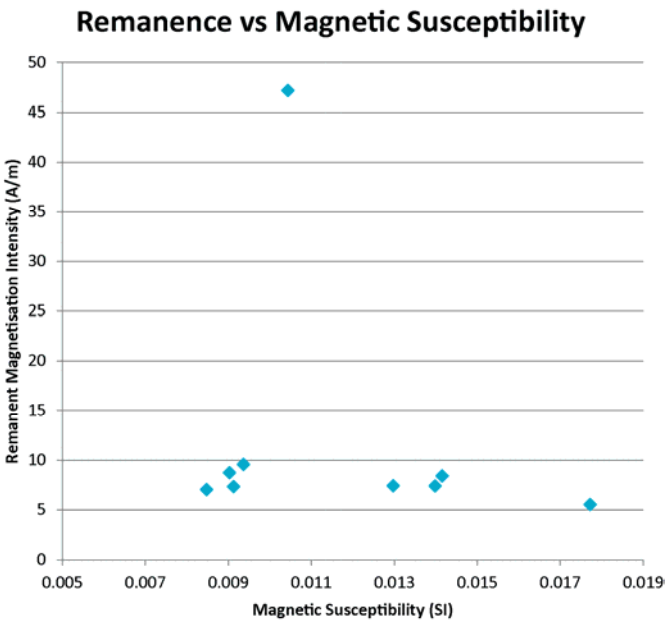

Figure 7: Lightning strikes typically cause remanent magnetisation intensity to increase by approximately 5 times the normal magnetisation, as demonstrated by these samples from the Giles Complex, Musgrave region, SA.

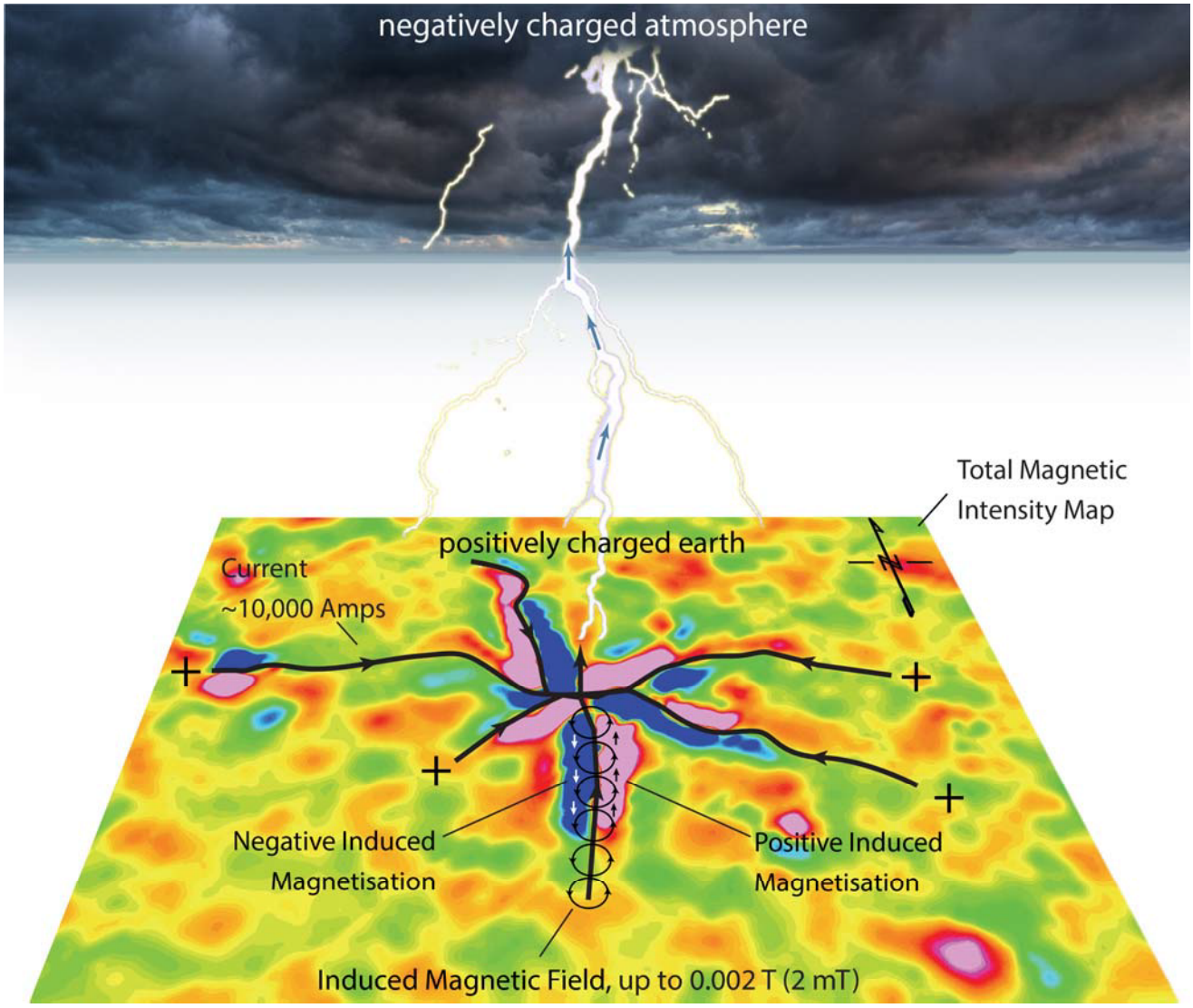

Figure 8: Schematic illustration a typical magnetic anomaly from a lightning strike (after Beard et al., 2009), and the mechanism by which the magnetisation is induced in the country rock.

The sudden and extreme current flow induced by the electric potential difference between the ground and atmosphere generates relatively strong local magnetic fields. A line current i produces a field intensity $H = i/2\pi r$ at a distance of r. So based on the data provided by Beard et al (2009), where i = 10,000 A, a field intensity of $10{,}000/(2\pi) = 1592$ A/m would be produced at a distance of 1 m from the strike. The corresponding flux density, calculated as $B = \mu_0 H = 1592 \times 4\pi \times 10^{-7}$ T = 0.002 T = 2000 μT, is equivalent to approximately 40 times the geomagnetic field. Such a field is sufficient to remagnetise grains with coercivities less than 2 mT (20 Oe) if they are unheated, or much more stable grains that are heated close to or above their Curie temperatures.

The gradient anomalies observed by Beard et al. (2009) ranged up to ~30 nT/m at a distance of ~2 m. If the the 1/r fall-off is taken into account, the corresponding field anomalies are about 60 nT at 2 m distance. This implies relatively low magnetisation of the soil adjacent to the current pathways, consistent with low concentrations of magnetic minerals in the test area. The anomalies observed by Beard et al. are way too small to deflect a compass needle by any discernible amount, so the fact

that compasses are profoundly disturbed over many lightning-affected outcrops of moderately magnetic rocks like basalts suggests that the test ground surface materials are not very magnetic. Hence, much larger anomalies are expected in rocks with high magnetite-content.

The current induces an electromagnetic field around the radial current flow, leading to anomalies of dual polarity, along the line of current flow (Fig 8). Because the IRM is a function of proximity but also orientation relative to the current, the enhanced remanent magnetisation intensity is often coupled with unusual magnetisation vectors that vary gradually away from the strike site and also show distinctive demagnetisation trends. Remanent magnetisation vectors of nearby samples will often start in several orientations and migrate toward a common orientation with successive demagnetisation steps (Fig 9). Because the current typically flows just beneath the surface we expect to observe mostly sub-horizontal magnetisation at the near surface, with locally consistent declinations. However, across a larger sampling area, great variance in the declinations is expected and these should be normal to the local current flow vector.

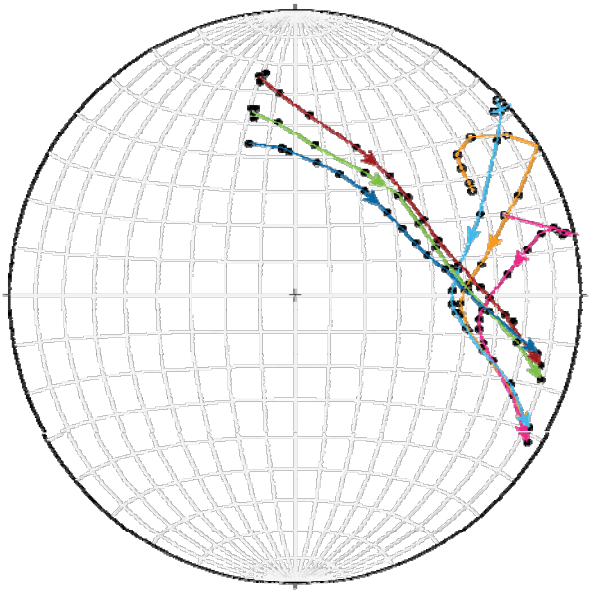

Figure 9: Illustrates typical demagnetisation behavior of lightning affected lithologies, demonstrated by samples from the Giles Complex

RELATING MAGNETIC FIELD INTERPRETATION TO SUB-SURFACE MAGNETIZATION MEASUREMENTS

In the previous sections we discussed challenges and pitfalls in recovering geologically-sourced magnetizations from palaeomagnetic samples. Note that when spurious DIM, IRM or PIM magnetizations are detected and dismissed, that still leaves us without an estimate of the direction and strength of NRM in the rock, which (together with its magnetic susceptibility) determines the resultant magnetization of the rock and thereby its external magnetic field. Furthermore, even if reliable NRM measurements are available it is still a considerable task to match those measurements to estimates derived from analysis or inversion of magnetic field data. The primary cause of this difficulty is the extreme variability of magnetization across a wide range of scales, compounded by extreme insufficiency of sampling. We illustrate these issues with a case study of the Rover 3 drill-hole near Tennant Creek in the Australian Northern Territory.

The Rover 3 anomaly and borehole

The Rover 3 magnetic anomaly (Figure 10) is a 2000 nT negative anomaly of approximately 1400 meters diameter detected on 8 north-south flight-lines of a regional aeromagnetic survey. The survey was flown at 200 meter line spacing and nominal 60 meter terrain clearance. The local geomagnetic field inclination is -52°. The anomaly occurs in a region of abundant gold mineralization, much of it associated with magnetite ironstone units.

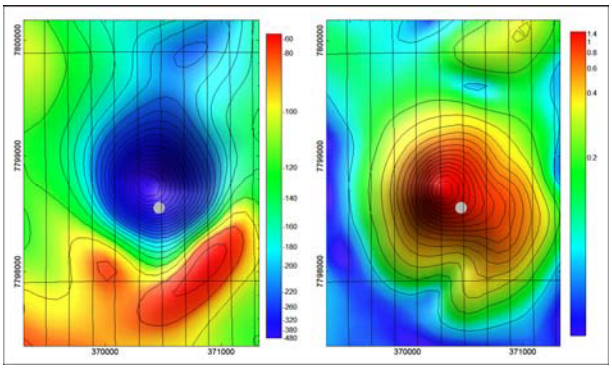

Figure 10: Rover 3 Anomaly (left) TMI and (right) total gradient of TMI. The grey point marks the Rover 3 Drill-hole location.

Castile Resources considered that the Rover 3 anomaly might be due to or be associated with mineralization and decided to drill-test it (Stephens, 2010). The approximately circular and almost purely negative anomaly provided a clear drilling location at or near its center, as confirmed by the total gradient transform of TMI, which maps the distribution of shallow magnetization with little sensitivity to its direction. The predicted depth to top of magnetization of 260 meters

(Stephens, 2010) was close to the actual depth (the report does not specify how that depth estimate was derived). The hole was planned to continue to a depth of 500 meters, but was extended to 738 meters because as reported (Stephens, 2010) "the moderate magnetism encountered in mafic units at the top of the hole is not considered to explain the large (inverse) magnetic anomaly". That interpretation was based on magnetic susceptibility measurements on the recovered core, although the anomaly was recognized as being due primarily to remanent magnetization. Austin and Foss (2014) subsequently inverted the anomaly and sampled the drill-core for palaeomagnetic measurements in an attempt to directly relate the magnetic anomaly to the sub-surface magnetization.

The magnetic field inversion

Figure 11 shows comparative images of TMI measured (left) and forward modelled from a plunging elliptic pipe model (right). The close match of the images confirms that the measured anomaly is closely matched by the source model. However, because all inverse solutions are non-unique, this alone does not prove the model correct. Figure 12 shows the model (blue) in perspective view, and Figure 13 shows the models as intersected on the central north-south flight-line.

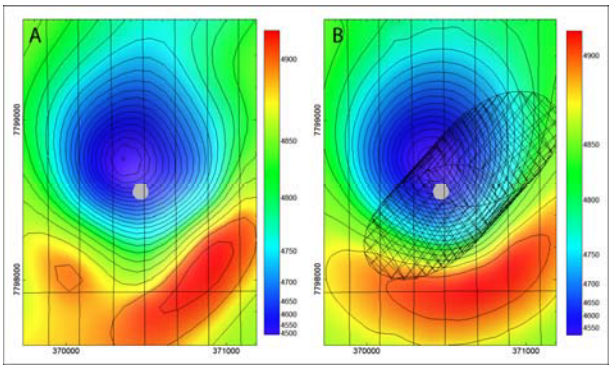

Figure 11: (left) measured TMI and (right) forward computed TMI from the best elliptic pipe model (shown in wireframe). The borehole location is above the modelled center of magnetization.

Figures 12 and 13 also include alternative models of different derived from independent inversions. These models (with very similar magnetic moments and magnetization directions) produce almost identical magnetic fields and it is not feasible to discriminate between them according to the fit of their computed fields to the measured anomaly. Each body has a homogeneous magnetization, which is all that can be justified at this distance from the magnetization. The two flat-topped models have predicted intersection depths at *ca.* 240 meters below surface, in good agreement with the drilling result (the ellipsoid model provides a less confident intersection depth which is slightly shallower than the drilling result).

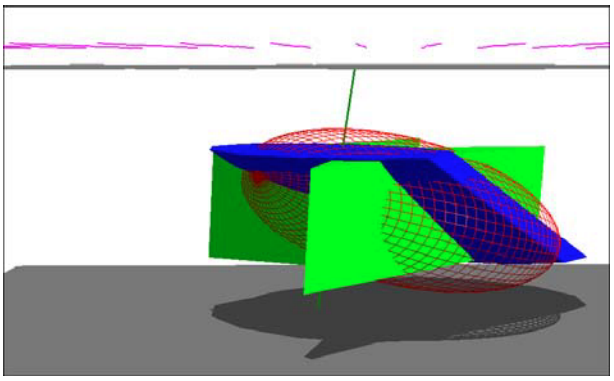

Figure 12: Perspective view of alternative source models (blue - elliptic pipe, green - polygonal section pipe, red - ellipsoid).

Bulk magnetization determination from drill-core

Figure 14 provides a graphic summary of density, magnetic susceptibility and remanent magnetization measurements made on samples from the Rover 3 core and their relationships to the major lithological units. These magnetization values were not available directly from the NRM measurements but required considerable effort to process and analyze, including exclusion of DIM and PIM magnetizations as described in the previous sections (details of the processing and analysis of the core magnetization measurements are available in Austin and Foss, 2014).

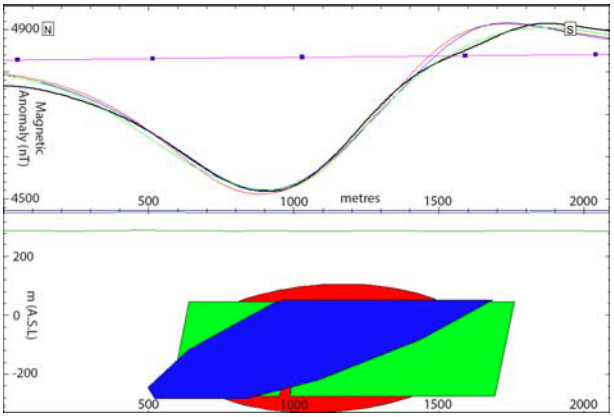

Figure 13: Section through the source models of Figure 12 along the central north-south flight-line.

The description of the lithology index is shown in Figure 15, which also includes tabulation of the simplified unit thicknesses, magnetic susceptibilities and remanent magnetizations.

Figure 14 shows that the Rover 3 Drill-hole intersected a mafic unit of approximately 13 meters thickness with high density, high magnetic susceptibility and strong remanent magnetization. The strong magnetization of this unit, together with the fact that it is the shallowest, give it a dominant contribution to the aeromagnetic anomaly. Although this unit has the highest magnetic susceptibilities measured, those susceptibilities are not sufficiently strong to explain the amplitude of the measured anomaly (and more significantly don't explain the negative amplitude of the anomaly). The anomaly is almost completely explained by the reverse remanent magnetization in the lower felsic volcanic units. These have ~10 times higher remanence relative to induced magnetization, as shown by the Koenigsberger ratio track in Figure 14. The Koenigsberger ratio is even higher for substantial depth intervals down the hole, but the absolute susceptibility and remanent magnetization values are much less, and so those magnetizations are less significant in generating the measured anomaly.

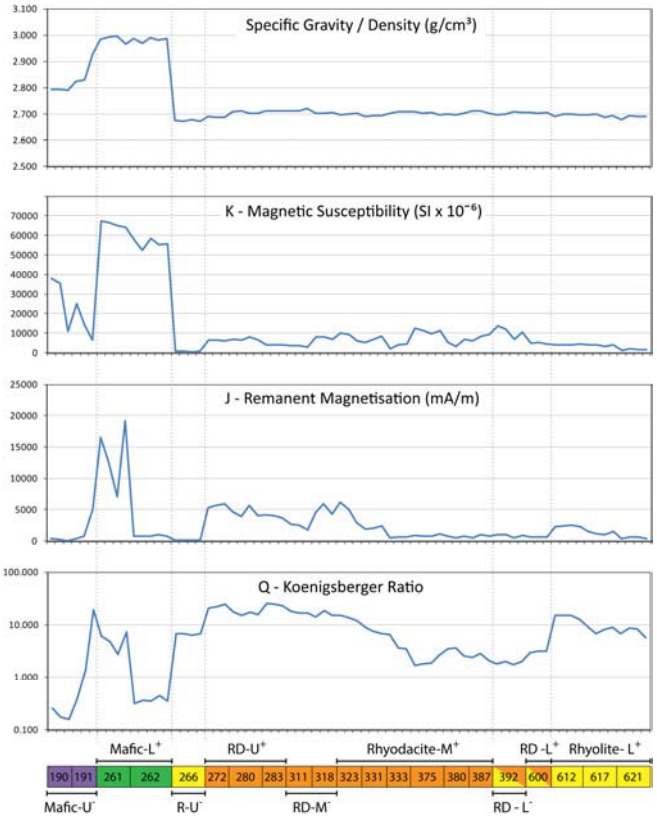

Figure 14: Summarized magnetization values down-hole with simplified lithology log.

Geological Unit as modelled	Top - m (b.s.l.)	Thick-ness (m)	MagSus (SIx10-6)	RemMag (mA/m)	Dec	Inc	Q
Rhyolite Upper - 1	-146	34	630	170	243	-53	6.7
Mafic Upper +	-112	13	21320	400	336.1	53.1	0.47
Rhyolite Upper - 2	-99	64	630	170	243	-53	6.7
Mafic Lower -	-35	6	60000	4000	174	-40.2	1.6
Rhyolite Upper - 3	-29	6	630	170	243	-53	6.7
Rhyodacite Upper +	-23	27	5600	4500	122	54.4	20
Rhyodacite Mid -	4	23	5200	3400	318	-43	25
Rhyodacite Mid +	28	68	7100	3200	99.5	42.3	11
Rhyodacite Lower -	96	110	10700	820	279	-45	19
Rhyolite Lower +	206	127	2900	1000	87.2	59.3	8.5
Rhyolite Lower ?	332	106	2000	800	267.2	-59.3	8.5

Figure 15: Simplified lithology log and tabulated magnetic susceptibility and remanent magnetization values.

The remanent magnetization directions derived from principal component analyses of the palaeomagnetic core measurements are plotted in Figure 16 together with the directions of resultant magnetization of the three inversion models. The close agreement of these two sets of directions (the mean values differ by only 11°) is consistent with the high Koenigsberger ratios. Inversion of the magnetic field data has therefore recovered a magnetization direction in close agreement with direct measurements (and the intersection depth has already been shown to closely match the model prediction).

Figure 17 shows a model of the distribution of magnetization that was generated by taking the spatial shell of the elliptic pipe inversion model, slicing it horizontally to represent each stratigraphic unit, and assigning those slices the magnetizations and magnetic susceptibilities estimated for the corresponding stratigraphic units (exact detail of how the magnetization values were assigned is described in Austin and Foss, 2014). The magnetic field forward computed from this model matches the observed anomaly to within 10% rms.

The homogeneous magnetization inversion model fits the data more closely, but that is because the model self-adjusts in the inversion process specifically to match the measured anomaly. There is little or no justification to adjust our sliced magnetization model to better fit the anomaly, which could be done in many ways by changing any combinations of the vertical distribution of magnetization in the slices and/or the horizontal extents and shapes of the slices (which are unconstrained by the single drill-hole).

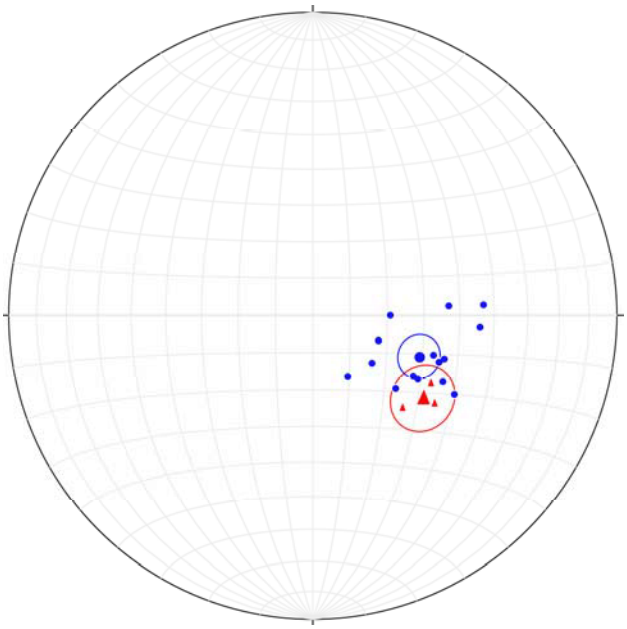

Figure 16: Remanent magnetization values from PCA of cleaned core measurements (blue) and from the 3 inversion models (red) with larger symbols showing mean directions and ellipses showing 95% confidence bounds (α95).

Figure 18 shows the derived magnetic model, which has been constrained by analyses of direct measurements of magnetization, and its spatial relationship to the Rover 3 magnetic anomaly. This model could not have been justified directly from any magnetic field inversion, which at the separation between magnetization and magnetic field measurements lacks the capability to resolve those vertically stacked magnetizations. Note also that for many geological systems the process of horizontally slicing a model and populating it with magnetizations measured in a single borehole would be poorly justified (e.g. for the studies presented earlier at the Cormorant and Artemis Deposits (Austin et al, 2016a, 2016b)) because the magnetization distribution may be much too complex to represent with any simple horizontally sliced model.

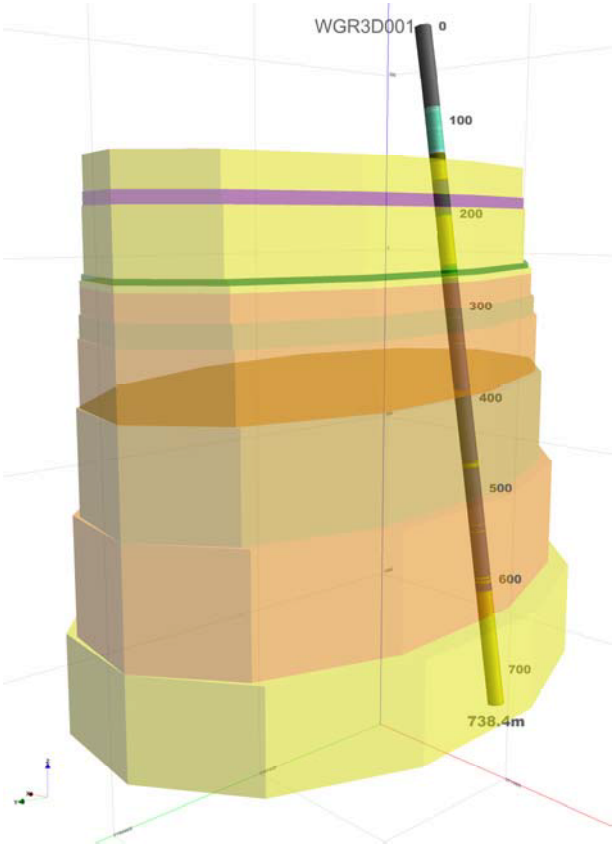

Figure 17: Rover 3 borehole with lithology coding and the 3D horizontal slice model derived to match that lithological layering.

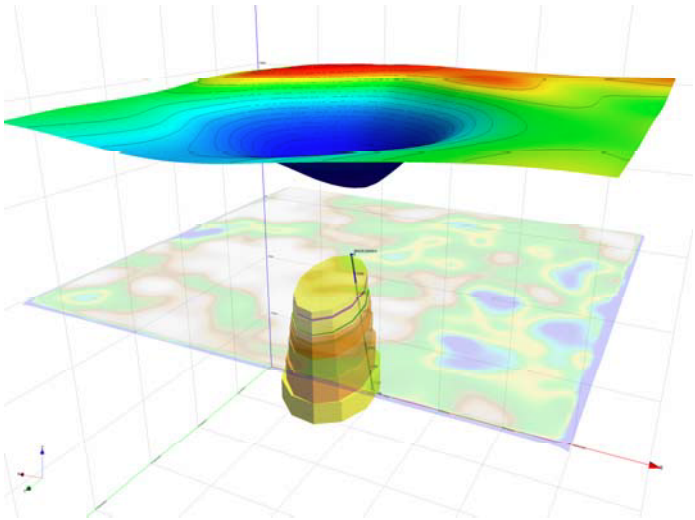

Figure 18: Illustration of the postulated horizontal zoning of measured magnetizations within an intrusive body as the cause of the Rover 3 aeromagnetic anomaly.

From the model shown in Figure 17 we can establish that much of the anomaly is matched from the field computed only from the shallow mafic units, demonstrating that extension of the borehole beneath that depth was poorly justified in testing any confident estimate of deeper magnetization. The guidance of laboratory-based remanent magnetization measurements would not have been timely enough to guide decision making while drilling at this remote site, but this shortcoming is addressed by a new instrument the 'Q-meter' (Schmidt and Lackie, 2014) which allows on-site low-resolution but rapid testing of remanent magnetization, susceptibility and thereby the Koenigsberger Ratio for strongly magnetized materials such as intersected at Rover 3. Potentially, with this instrument, the drilling could have been terminated at much shallower depth, saving considerable costs.

CONCLUSIONS

We have presented some of the impediments to directly measuring geological remanent magnetizations due in particular to drilling induced remanence, lightning strikes and re-magnetization by pencil magnets, and have shown how those spurious magnetizations can be recognized and removed. Unfortunately this still leaves us without a sound estimate of the NRM of the rock before those magnetizations were acquired, and which would hopefully characterize the undisturbed rock still in the ground. There are also considerable challenges from what is invariably a sparse sampling of magnetization, which is a property that can vary by orders of magnitude across small and large distances. We show with a case study of the Rover 3 magnetic anomaly and borehole near Tennant Creek Australia, that for relatively simple geology (an apparently horizontally dominated distribution of magnetization) the assumptions imposed by analysis of magnetic field data at considerable distance from a magnetization do not preclude creation and selection of models which provide a reasonable and useful representation of sub-surface geology.

REFERENCES

Audunsson H. and Levi, S., 1989. Drilling-induced remanent magnetization in basalt drill cores. Geophys. J. Int. 98 (3): 613-622.

Austin, J.R., and Foss, C.A., 2014. The paradox of scale: reconciling magnetic anomalies with rock magnetic properties for cost-effective mineral exploration, J. Appl. Geophysics, 104, 121-133.

Austin, J.R., Gazley, M.F., Patterson, B., leGras, M., Walshe, J.L., 2016a. Uncover Cloncurry – The Cormorant Cu-Au Prospect: Integrated Petrophysical and Geochemical analyses. CSIRO, Australia, pp. 44.

Austin, J.R., Gazley, M.F., Patterson, B., leGras, M., Walshe, J.L., 2016b. The Artemis Zn-Cu deposit: Integrated Petrophysical and Geochemical analyses. CSIRO report number EP165035, Australia, pp. 45.

Austin, J., Schmidt, P. and Lilly, R., 2013. Anisotropy of Magnetic Susceptibility (AMS) and Paleomagnetism applied to the differentiation of structural and metallogenic controls on Iron Oxide Copper-Gold (IOCG) mineralisation: a case study from Monakoff, NW Queensland. ASEG Extended Abstracts 2013 (1), 1-5.

Beard, L.P., Norton, J. and Sheehan J.R., 2009. Lightning-Induced Remanent Magnetic Anomalies in Low-Altitude Aeromagnetic Data. Journal of Environmental and Engineering Geophysics, 14(4), 155-161.

De Wall, H. and Worm, H.-U., 2001. Recognition of drilling-induced remanent magnetization by Q-factor analysis: a case study from the KTB-drillholes. J. Appl. Geophys. 46, 55–64.

Schmidt, P.W., and Lackie, M.A., 2014. Practical consideration: making measurements of susceptibility, remanence and Q in the field. Exploration Geophysics, 45(4) 305-313

Stephens, D., 2010. Geophysics and drill collaboration report-EL25511: Northern Territory Exploration Report R2010-20 10.